Article

In vitro DNA Adduction Resulting from Metabolic Activation of Diosbulbin B and 8-Epidiosbulbin E Acetate

Dongju Lin, Weiwei Li, Xutong Tian, Ying Peng, and Jiang Zheng

Chem. Res. Toxicol., **Just Accepted Manuscript** • DOI: 10.1021/acs.chemrestox.8b00071 • Publication Date (Web): 06 Dec 2018

In vitro DNA Adduction Resulting from Metabolic Activation of Diosbulbin B and 8-Epidiosbulbin E Acetate

Dongju Lin,[†] Weiwei Li,[‡] Xutong Tian,[†] Ying Peng,[§*] and Jiang Zheng[‡§*]

[‡]State Key Laboratory of Functions and Applications of Medicinal Plants, Key Laboratory of Pharmaceutics of Guizhou Province, Guizhou Medical University, Guiyang, Guizhou, 550025, P.R.China; [†]Key Laboratory of Pharmaceutical Quality Control of Hebei Province, Baoding 071002, China; College of Pharmaceutical Sciences, Hebei University, Baoding 071002, China;[§]Wuya College of Innovation, Shenyang Pharmaceutical University, Shenyang, Liaoning, 110016, P.R.China.

Running title:

Identification of DNA adducts of DBB and EEA

Corresponding Authors:

Jiang Zheng, PhD
Wuya College of Innovation, Shenyang Pharmaceutical University, Shenyang, Liaoning, 110016, P. R. China
State Key Laboratory of Functions and Applications of Medicinal Plants, Key Laboratory of Pharmaceutics of Guizhou Province, Guizhou Medical University, Guiyang, Guizhou, 550025, P.R. China

Email: zhengneu@yahoo.com
Tel: +86-24-23986361; Fax: +86-24-23986510

‡, § : The two corresponding units contributed equally to this work.

Ying Peng, PhD
Wuya College of Innovation, Shenyang Pharmaceutical University, Shenyang, Liaoning, 110016, P. R. China
Email: yingpeng1999@163.com
Tel: +86-24-23986361; Fax: +86-24-23986510

TOC Graphic

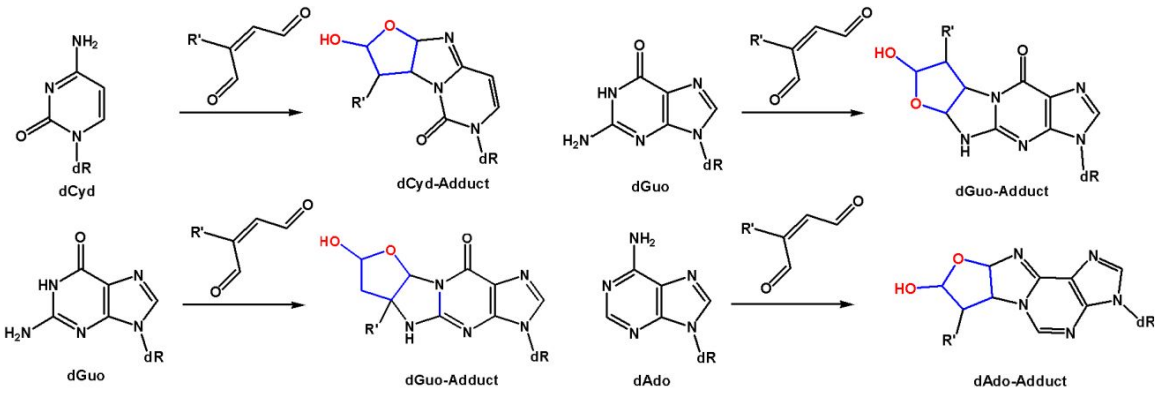
dCyd
dCyd-Adduct
dGuo
dGuo-Adduct
dGuo
dGuo-Adduct
dAdo
dAdo-Adduct

Abstract

Diosbulbin B (DBB) and 8-epidiosbulbin E acetate (EEA), belonging to furan-containing diterpenoid lactones, are the primary components of *Dioscorea bulbifera* L. (DB), a traditional Chinese medicine herb. Our earlier studies indicated that consumption of DBB or EEA induced acute hepatotoxicities. Both DBB and EEA were bioactivated by P450 3A4 to generate the corresponding *cis*-enedial reactive metabolites which are associated with the hepatotoxicities. It has been proposed that the electrophilic intermediates attack cellular nucleophiles such as protein or DNA, thought to be a mechanism of triggering toxicities. The purpose of our present study were to define the interaction of the electrophilic reactive metabolites originating from DBB and EEA with 2'-deoxyguanosine (dGuo), 2'-deoxycytidine (dCyd), and 2'-deoxyadenosine (dAdo) and to characterize DNA adducts arising from the reactive metabolites of DBB and EEA. The reactive metabolites of DBB and EEA were found to covalently bind to the exocyclic and endocyclic nitrogens of dCyd, dGuo, and dAdo to generate oxadiazabicyclo[3.3.0]octaimine adducts. The reactive metabolites of DBB and EEA also attacked dGuo, dAdo, and dCyd of calf thymus DNA. The DNA adducts possibly contribute to the toxicologies of DBB and EEA.

Introduction

Dioscorea bulbifera L. (DB), known as Huang-Yao-Zi in Chinese, belongs to a member of the yam family *Dioscoreaceae*.[1] It is widely employed to treat carbuncles, lung abscesses, breast lumps, and goiter in China.[2] Additionally, DB possesses a series of pharmacological properties, including antitumor,[3] antifeedant,[4] anti-inflammation,[5] and anti- salmonellal activities.[6] DB and related remedies are often used for the treatment of thyroid gland diseases and a variety of tumors.[7-8] It has been reported that DB has a wide variety of therapeutical values, but the adverse effects of DB have also attracted attention so that this medicinal herb can be consumed safely.[9] Many cases of hepatitis have been reported to be related with the consumption of DB and even deaths due to fulminant hepatic failure since 1976.[10,11] Animal studies demonstrated that oral consumption of ethanol extracts of DB caused increases in serum alanine transaminase (ALT), aspartate transaminase (AST), and lipid peroxide in hepatic tissues of mice.[12] DB contains varieties of diterpenoid lactones,[13] and diosbulbin B (DBB; Scheme 1) has been identified as the one in a great abundance among the diterpenoid lactones.[14] In addition, our preliminary study found that the content of 8-epidiosbulbin E acetate (EEA; Scheme 1) varied largely in DB and the quantity of EEA in DB relied on the commercial source.[15] We found that both DBB and EEA were capable of inducing acute liver injury.[15] EEA was much more hepatotoxic than DBB.[16] Both DBB and EEA contain a 3-substituted furan ring. Our preliminary study demonstrated that both DBB and EEA were metabolized by cytochrome P450 3A4 to *cis*-enedial intermediates (**1** and **2**; Scheme 1)

which are responsible for the hepatotoxicities of DBB and EEA.[15,17] *cis*-Enedial, an electrophilic intermediate, is chemically reactive to nucleophiles, and it easily alkylates protein, polyamine, and DNA nucleophiles, which were considered to be a significant mechanism of toxicities.[18-21] Our previous study manifested that the reactive intermediates of DBB and EEA could react with cysteine and lysine residue(s) of hepatic proteins to form protein adducts. Furthermore, the protein covalent binding was correlated with the hepatotoxicities of DBB and EEA.[22,23]

Furan is metabolized to form a chemically reactive metabolite of *cis*-2-butene-1,4-dial (BDA) mediated by cytochrome P450 2E1. It is suggested that this metabolite possibly reacts with proteins to induce cytotoxicity or attacks the exocyclic and endocyclic nitrogens of dCyd, dGuo, and dAdo to generate diastereomeric oxadiazabicyclo[3.3.0]octa-imine adducts.[18,24] It has been documented that furan could bind to DNA in the target organ of furan carcinogenicity.[25] DNA covalent binding has been thought to be another significant action to trigger toxicities. We hypothesized that the reactive intermediates of DBB and EEA can covalently bind to DNA, which may be relevant with hepatotoxicities induced by DBB and EEA. As a consequence, the present study aimed at the determination of the potential of reactive intermediates derived from DBB and EEA to covalently bind to DNA.

Materials and methods

Reagents

Diosbulbin B (DBB) and 8-epidiosbulbin E acetate (EEA) were separated and purified from DB rhizomes in our laboratory, based on previously reported procedures.[26,27] The structures were affirmed by mass spectrometry and NMR. The purities of DBB and EEA were >98% assessed via high-performance liquid chromatography (HPLC). 2'-Deoxyadenosine (dAdo), 2'-deoxycytidine (dCyd), 2'-deoxguanosine (dGuo), thymine, DNase I, alkaline phosphatase, phosphodiesterase I, and calf thymus DNA were purchased from Sigma (St. Louis, MO). All organic solvents were purchased from Fisher Scientific (Springfield, NJ) with analytical or HPLC grade.

Synthesis of dimethyldioxirane (DMDO)

Dimethyldioxirane (DMDO) was prepared, according to previously published method [28]. In brief, 30 mL of acetone and 0.285 mol of $NaHCO_3$ were mixed in a 1L round bottom flask containing 20 mL of distilled H_2O and cooled in an water/ice bath with stirring. After 20 min, stirring was halted, followed by addition of Oxone (25 g, 0.041 mol). The resultant mixture was stirred for 15 min, and then a slight vacuum was applied to the reaction assembly. The resulting pale yellow distillate was condensed in a receiving flask, followed by cooling in an acetone/dry ice bath. The concentration of DMDO was determined by titration, according to a reported method.[29] The concentration DMDO ranged from 0.06 to 0.065 M.

Synthesis of DBB/EEA-derived dCyd, dAdo, and dGuo adducts

DBB (10 mg, 0.029 mmol) or EEA (10 mg, 0.026 mmol) dissolved in 2.0 mL acetone was cooled in a dry ice bath for 1 min. The pre-prepared DMDO solution (4 mL) was dropwise added to the individual reactant solution with stirring, and the mixture was stirred for 10 min. The reaction mixture was placed at room temperature and left to stand for 1 h. The unreacted DMDO was removed by blowing with nitrogen gas. To the resulting mixture was dCyd, dAdo, or dGuo (20 mg for each) dissolved in PBS (2 mL, 0.1 M) added dropwise, respectively. After 1 h stirring at 60 °C, the reaction mixture was concentrated under a stream of nitrogen gas at room temperature. The resultant solution was kept at -80 °C until purification. The synthetic DBB-derived dCyd, dGuo, and dAdo adducts were purified by a semipreparative HPLC system.

The synthetic products were isolated and purified by a reverse phase–HPLC system using a YMC-Pack ODS-A C18 column (250 × 10 mm, 5 μm; YMC Technologies, Japan, CA). The column temperature was set at 25 °C. The column was eluted with a mobile phase system composed of water with 0.1% formic acid and 25% acetonitrile at a flow rate of 1.6 mL/min. The eluents were monitored at 210 and 254 nm. The structures of purified products were determined by mass spectrometry and ^{1}H NMR. The purity of DBB-derived dCyd, dAdo, and dGuo adducts (Scheme 2) was >96%, based on HPLC analysis.

^{1}H NMR (DMSO-d_6, 600MHz) of DBB-derived dCyd adduct: δ1.10 (3H, s, H-17), 1.52 (2H, m, H-1”), 1.74 (2H, d, J=11Hz,H-3”), 1.93 (1H, m, H-5”), 2.14 (2H, m, H-7”), 2.21 (2H, m,H-11”), 2.24 (1H, m, H-2’), 2.39 (1H, m, H-13”), 2.45 (1H, m,

H-10”), 2.80 (1H, d, *J*=4.3 Hz,H-4"), 3.53 (2H, m, H-5’), 3.80 (1H, m, H-4’), 4.21 (1H, m, H-3’) , 4.54 (1H, m, H-7), 4.61 (1H, m, H-12”), 4.72 (1H, m, H-6”), 4.76 (1H, dd, *J*=5.3, 5.3 Hz, H-2”), 5.00 (1H, br s, H-5’OH), 5.20 (1H, br s, H-3’OH), 5.42 (1H, br s, H-14”), 5.76 (1H, m, H-5), 5.98-5.84 (1H, m, H-8), 6.15 (1H, m, H-1’), 7.45 (1H, m, H-4); ^{13}C (DMSO-d_6, 150MHz): δ15.96 (C-17”), 28.58 (C-1”), 29.26 (C-2’), 36.19 (C-10”), 37.12 (C-7”), 38.43 (C-13”), 39.24 (C-3”), 40.58 (C-11”), 42.12 (C-5”), 42.30 (C-4’’), 45.63 (C-9”), 59.35 (C-7), 61.93 (C-5’), 65.78 (C-12”), 71.20 (C-3’), 76.85 (C-2”), 78.54 (C-6”), 83.01 (C-4’),87.51 (C-1’), 96.50 (C-5), 98.96 (C-14”), 101.15 (C-8), 138.20 (C-4), 175.80 (C-16”), 176.71 (C-15”).

^{1}H NMR (DMSO-d_6, 600MHz) of DBB-derived dGuo adduct: δ1.08 (3H, s, H-17), 1.48 (2H, m, H-1”), 1.72 (2H, d, *J*=11Hz,H-3”), 1.96 (1H, m, H-5”), 2.11 (2H, m, H-7”), 2.20 (2H, dd, *J*=11, 11.9 Hz,H-11”), 2.23 (1H, m, H-2’), 2.34 (1H, m, H-13”), 2.48 (1H, m, H-10”), 2.50 (1H, m, H-2’), 2.79 (1H, d, *J*=4.1 Hz,H-4”), 3.61-3.42 (2H, m, H-5’), 3.80 (1H, m, H-3’), 4.31(1H, m, H-4’) , 4.56 (1H, m, H-12”), 4.73 (1H, m, H-6”), 4.78 (1H, dd, *J*=5.3, 5.3 Hz, H-2”), 4.88 (1H, br s, H-5’OH), 4.90 (1H, m, H-7), 5.19 (1H, br s, H-3’OH), 5.45 (1H, br s, H-14”), 6.10 (1H, m, H-1’), 7.17 (1H, br s, H-6), 7.82 (1H, s, H-2); ^{13}C (DMSO-d_6, 150MHz): δ 15.98 (C-17”), 28.60(C-1”), 29.27 (C-2’), 36.20 (C-10”), 37.15 (C-7”), 38.46 (C-13”), 39.21 (C-3”), 40.53 (C-11”), 42.15 (C-5”), 42.33 (C-4”), 45.61 (C-9”), 59.30 (C-7), 61.80 (C-5’), 65.74 (C-12”), 70.53 (C-3’), 76.83 (C-2”), 78.10 (C-6”), 84.91 (C-1’), 86.27(C-4’), 88.23 (C-6), 90.12 (C-8”), 98.10 (C-14”), 138.59 (C-2),175.89 (C-16”), 176.74 (C-15”).

^{1}H NMR (DMSO-d_6, 600MHz) of DBB-derived dAdo adduct: δ1.12 (3H, s, H-17), 1.52(2H, d, *J*=5.5, 5.5 Hz, H-1”), 1.84 (2H, d, *J*=10.6, 11.0 Hz,H-3”), 1.98 (1H, m, H-5”), 2.21 (2H, m, H-7”), 2.24 (2H, dd, *J*=11.2, 11.6 Hz,H-11”), 2.26 (1H, m, H-2’), 2.25 (1H, m, H-13”), 2.53 (1H, m, H-10”), 2.60 (1H, m, H-2’), 2.81 (1H, d, *J*=4.3 Hz,H-4”), 3.61 (2H, m, H-5’), 3.80 (1H, m, H-4’), 4.31 (1H, m, H-3’) , 4.59 (1H, m, H-12”), 4.83 (1H, m, H-6”), 4.75 (1H, m, H-7), 4.89 (1H, dd, *J*=5.5, 5.5 Hz, H-2”), 4.95 (1H, br s, H-5’OH), 5.30 ((1H, m, H-14”), 5.36 (1H, br s, H-3’OH), 6.00 (1H, m, H-8), 6.17 (1H, m, H-1’), 8.16 (1H, s, H-2), 8.29 (1H, s, H-5); ^{13}C (DMSO-d_6, 150MHz): δ 16.37 (C-17”), 29.68 (C-1”), 31.54 (C-2’), 38.67 (C-13”), 37.20 (C-7”), 39.29 (C-3”), 40.63 (C-11”), 40.95 (C-10”), 42.21 (C-5”), 42.42 (C-4”), 45.82 (C-9”), 58.90 (C-7), 61.54 (C-5’), 65.84 (C-12”), 70.97 (C-3’), 77.54 (C-2”), 78.31 (C-6”), 84.89 (C-1’), 87.39 (C-4’), 90.35 (C-8”), 90.94 (C-8), 100.45 (C-14”),139.31 (C-2), 141.25 (C-5), 175.92 (C-16”), 176.86 (C-15”).

Preparation of calf thymus DNA adducts derived from reactive metabolites of DBB/EEA

The oxidized products of DBB and EEA prepared in accordance with the above methods were individually mixed with ctDNA (0.3 mg dissolved in 500 μL of 50 mM potassium phosphate, pH 7.4) at 37 °C for 8 h.

DNA hydrolysis

The resulting mixtures above were enzymatically hydrolyzed at 37 °C for 15 h with a mixture of phosphodiesterase I (10 mg/mL), alkaline phosphatase (10 mg/mL),

and DNase I (1.0 mg/mL) in a 1.0 mL solution of 5.0 mM $CaCl_2$ and 5.0 mM $MgCl_2$. The mixtures were centrifuged at 19,000g for 10 min. The supernatants were enriched by solid phase extraction (Strata-X 30 mg cartridges, Phenomenex), eluted with sequential water, 20% methanol, and 100% methanol (1 mL each). The resulting eluents were then pooled and concentrated to about 100 μL under reduced pressure. Analysis of the digestion mixture was performed using LC-MS/MS.

LC-MS/MS Analysis

An SCIEX Instruments 4000 Q hybrid triple quadrupole-linear ion trap mass spectrometer (Applied Biosystems, Foster City, CA, USA) was equipped with an Agilent 1260 Series Rapid Resolution LC system. In order to acquire the accurate mass of the analytes, a microQ-TOF MS (Bruker Co., Karlsruhe, Germany) was employed. A Symmetry reverse-phase C18 column of Waters with 3.5 μm particle size and 4.6 × 150 mm i.d. (Waters, Milford, MA), was employed for chromatographic separation with an elution gradient system consisting of acetonitrile with 0.1% formic acid as mobile phase A and water with 0.1% formic acid as mobile phase B. The gradient started with 10% A for 2 min, linearly increased to 90% A in 8 min, kept constant at 90% A for 2 min, and switched back to 10% A in 2 min. The HPLC flow rate was set at 0.8 mL/min and the column was eluted at room temperature. The Q TRAP^{TM} mass spectrometer was operated in positive ion mode. The curtain gas was set at 20 psi, GA1 and GA2 were set at 50 psi, the source temperature was set at 650 °C. In order to accomplish the highest sensitivity possible, the main mass parameters were optimized in the MRM mode, such as

declustering potential (DP), collision energy (CE), and collision cell exit potential (CXP).. The representative ion pairs (corresponding to DP; CE; CXP) were *m/z* 588→472 (110, 40, 13) for DBB-derived dCyd adduct, *m/z* 610→494 (110, 40, 13) for DBB-derived dGuo adduct, *m/z* 594→478 (110, 40, 13) for DBB-derived dAdo adduct, *m/z* 632→456 (110, 40, 13) for EEA-derived dCyd adduct, *m/z* 654→478 (110, 40, 13) for EEA-derived dGuo adduct and *m/z* 638→462 (110, 40, 13) for EEA-derived dAdo adduct. MS/MS spectra for adducts can be acquired using the information-dependent acquisition (IDA) of the enhanced product ion (EPI). IDA threshold was set at 5000 counts per second (cps) for the MRM scan. EPI scan rate was 1000 amu/s and the scan for product ions ranged from 50 to 700 amu. CE was set at 35 eV with a CE spread of 10 eV. Dynamic exclusion, defining the time for exclusion of former target ions after acquiring an EPI scan, was set at 10 s after 3 occurrences to allow the detection of coeluting substances. SCIEX Analyst™ software (versions 1.6 and 1.6.2) was employed for data acquisition and processing.

.

Results

Formation of DBB-derived dCyd, dGuo, and dAdo adducts.

DBB was oxidized by DMDO to produce *cis*-enedial reactive intermediate **1** which reacted with dCyd, dGuo, or dAdo. Mass spectrometric analysis (positive mode) detected DBB-derived three adducts **(**A1-A3**)** in the microsomal reactions. Adduct A1 determined by scanning ion pair of *m/z* 588→472 eluted at 6.69 min (Figure 1A). Collision-induced dissociation (CID) of *m/z* 588 produced *m/z* 472 through neutral loss of 116 Da, suggesting the loss of 2'-deoxyribose (Figure 1C). High resolution MS of A1 revealed exact *m/z* of 588.2168, responsible for the molecular formula of $C_{28}H_{34}N_3O_{11}$ within 5 ppm (Table S1). NMR analysis showed that the formation of DBB-derived dCyd adduct [^{1}H δ7.45 (m, H-4), 5.98-5.84 (m, H-8), 5.76 (m, H-5), 5.42 (m, H-14''), 4.54 (m, H-7); ^{13}C δ138.20 (C-4), 101.15 (C-8), 98.96 (C-14"), 96.50 (C-5), 59.35 (C-7)] (Table S3). Additionally, the ^{1}H and ^{13}C NMR data showed that the existence of 2'-deoxyribose [^{1}H δ6.15 (m, H-1'), 5.20 (br s, H-3'OH), 5.00 (br s, H-5'OH), 4.21 (m, H-3'), 3.75 (m, H-4'), 3.53 (m, H-5'),2.24 (m, H-2'); ^{13}C δ87.51 (C-1'), 71.20 (C-3'), 83.01 (C-4'), 61.93 (C-5'), 30.80 (C-2')] (Table S3). This led us to proposing that A1 resulted from the reactive intermediate of DBB conjugated with one molecule of dCyd (Scheme 3).

Although a peak of adduct A2 at *m/z* 628 representing $[M+H]^+$ was not detected in the Q1 mass spectrum, the mass at *m/z* 610 was assigned to $[M+H - H_2O]^+$ ions. Adduct A2 determined by scanning ion pair *m/z* 610→494 eluted at 6.75 min (Figure 2A). The product ion (MS^2) spectrum of adduct A2 (Figure 2C), obtained via

MRM-EPI scanning, contained the indicative characteristic fragment ion at *m/z* 494 which was derived from the neutral loss of 2'-deoxyribose (Figure 2C). Further analysis by LC/Q-TOF MS showed $[M+H - H_2O]^+$ of adduct A2 at *m/z* 610.2120, corresponding to the formula of $C_{29}H_{32}N_6O_{10}$ (Table S1). NMR analysis confirmed the formation of adduct A2 [^{1}H δ2.34 (m, H-13''), 5.45 (br s, H-14''), 7.82 (s, H-2), 8.96 (s, H-5), 7.17 (br s, H-6),4.90 (m, H-7) , ^{13}C δ38.46 (C-13''), 98.10 (C-14"), 138.59 (C-2), 88.23 (C-6), 59.30 (C-7)] (Table S4). In addition, the ^{1}H and ^{13}C NMR data demonstrated that the existence of 2'-deoxyribose [^{1}H δ6.10 (m, H-1'), 5.19 (br s, H-3'OH), 4.88 (br s, H-5'OH), 3.80 (m, H-3'), 4.31 (m, H-4'), 3.61-3.42 (m, H-5'), 2.50 (m, H-2'), 2.23 (m, H-2'); ^{13}C δ84.91 (C-1'), 70.53 (C-3'), 86.27 (C-4'), 61.80 (C-5'), 29.27 (C-2')] (Table S4). On the basis of the observed mass spectrometric and NMR data, we propose that A2 was composed of the reactive intermediate of DBB and one molecule of dGuo (Scheme 3).

We failed to find adduct A3 at *m/z* 612 representing $[M+H]^+$ in positive mode. Instead, the adduct was detected by scanning of ion at *m/z* 594 responsible for $[M+H - H_2O]^+$ ion. . Adduct A3 determined by scanning ion pair *m/z* 594→478 eluted at 7.64 min (Figure 3A). Product ion (MS^2) spectrum of adduct A3 revealed a characteristic product ion at *m/z* 478, originating from the loss of 2'-deoxyribose (-116Da) (Figure 2C). LC-Q-TOF MS further demonstrated $[M+H - H_2O]^+$ at *m/z* 594.2180 (Table S1), corresponding to the formula of $C_{29}H_{32}N_5O_9$ (Table S1). NMR analysis confirmed the formation of adduct A3 [^{1}H δ5.30 (m, H-14''), 2.25 (m, H-13''), 8.16 (s, H-2), 8.29 (s, H-5), 4.75 (m, H-7), 6.00 (m H-8); ^{13}C δ100.45 (C-14"), 38.67 (C-13"),

139.31 (C-2), 141.25 (C-5), 58.90 (C-7), 90.94 (C-8)] (Table S5). Additionally, the ^{1}H and ^{13}C NMR data demonstrated that the existence of 2'-deoxyribose [^{1}H δ6.17 (m, H-1'), 5.36 (br s, H-3'OH), 4.95 (br s, H-5'OH), 4.31 (m, H-3'), 3.80 (m, H-4'), 3.61 (m, H-5'), 2.60 (m, H-2'), 2.28 (m, H-2'); ^{13}C δ84.89 (C-1'), 70.97 (C-3'), 87.39 (C-4'), 61.54 (C-5'), 31.54 (C-2)] (Table S5). The observed mass spectrometric and NMR data suggest that A3 consisted of the reactive intermediate of DBB and one molecule of dAdo (Scheme 3).

Formation of DBB-*cis*-enedial calf thymus DNA adducts

To determine the reactivity of the reactive intermediate of DBB to DNA, the synthetic oxidative products of DBB was incubated with calf thymus DNA as a model DNA. The reaction mixture was hydrolyzed using DNase I, alkaline phosphatase, and phosphodiesterase I. The resultant mixtures were analyzed as described above. Three adducts were observed in the digestion mixture. These adducts showed the same chromatographic behaviors as synthetic DBB-derived dCyd, dGuo, and dAdo adducts (Figure 1B-3B), respectively. This indicates that the reactive intermediate of DBB could covalently bind to calf thymus DNA.

Formation of EEA-derived dCyd, dGuo, and dAdo adducts.

EEA was oxidized by DMDO to generate the corresponding *cis*-enedial reactive intermediate (**2**), followed by reaction with dCyd, dGuo, and dAdo individually. Mass spectrometric analysis showed three adducts **(**A4-A6**)** formed in the reaction mixtures.. Adduct A4 determined by scanning ion pair of *m/z* 632→456 eluted out

at 6.93 min (Figure 4A). Collision-induced dissociation (CID) of *m/z* 632 produced *m/z* 516 through the neutral loss of 116 Da, suggesting the loss of 2'-deoxyribose (Figure 4C). The major fragment ion at *m/z* 456 is proposed to originate from further loss of CH_3COOH from EEA (Figure 4C). Further analysis of A4 by LC/Q-TOF MS demonstrated exact molecule ion of 632.2423, which is in agreement with the formula of $C_{30}H_{38}N_3O_{12}$ (Table S2). This indicates that A4 resulted from the reactive intermediate of EEA which is conjugated with one molecule of dCyd (Scheme 4).

Q1 full scanning of *m/z* 654 in positive mode allowed us to observe adduct A5, considered to represent $[M + H - H_2O]^+$. Adduct A5 monitored by scanning ion pair *m/z* 654→478 eluted out at 7.46 min (Figure5A). The MS/MS spectrum of A5 revealed the major fragment ions arising from the neutral loss of 2'-deoxyribose,generating the product ion at *m/z*538 (Figure 5C). The major fragment ion at *m/z* 478 is proposed to originate from the further neutral loss of CH_3COOH from EEA (Figure 5C). Further analysis of adduct A5 by LC/Q-TOF MS displayed its molecular ion $[M + H - H_2O]^+$ at *m/z* 654.2387, responsible for the formula of $C_{31}H_{36}N_5O_{11}$ (Table S2). On the basis of the observed mass spectrometric data, we propose that A5 was composed of the reactive intermediate of EEA and one molecule of dGuo (Scheme 4).

Adduct A6 was determined by Q1 full scanning of *m/z* 638 in positive mode, considered to represent $[M + H - H_2O]^+$. Adduct A6 monitored by scanning ion pair *m/z* 638→462 eluted out at 8.51 min (Figure 6A). The MS/MS spectrum of adduct

A6 exhibited a product ion at *m/z* 522, suggesting the loss of 2'-deoxyribose (116 Da) (Figure 6C). The major fragment ion at *m/z* 462 is proposed to originate from the loss of CH_3COOH from EEA and the elimination of 2'-deoxyribose from the protonated molecular ion (Figure 6C). High resolution mass spectrometric analysis of adduct A6, exhibited molecular ion $[M + H- H_2O]^+$ at *m/z* 638.2410 (Table S2), corresponding to the formula of $C_{31}H_{36}N_5O_{10}$ (Table S2). This indicates that A6 was generated through conjugation of the reactive intermediate of EEA with one molecule of dAdo (Scheme 4).

Characterization of EEA-*cis*-enedial calf thymus DNA adducts

Similar experiments were performed to determine adduction of calf thymus DNA by the reactive intermediate of EEA as that for DBB. Three adducts were detected in the digestion mixture.As expected, these adducts displayed the same chromatographic properties as respective EEA-derived dCyd,dGuo adduct, and dAdo adducts (Figure 4B-6B) synthesized, indicating that the reactive intermediate of EEA could covalently modify calf thymus DNA.

Discussion

Hepatotoxicities of DB have been well documented in experimental animals and humans.[10-12] DBB has been reported to be the primary diterpenoid lactone in DB.[14] In addition, we found that EEA was a dominant diterpenoid lactone in some varieties of DB, and its content varied from one source of DB to another.[15] Our earlier study demonstrated both DBB and EEA could cause severe liver injuries.[16,30] DBB and EEA were biotransformed to the corresponding *cis*-enedial intermediates (**1** and **2**; Scheme 1), and the formation of the electrophilic intermediates was associated with the hepatotoxicities of DBB and EEA.[16,30] Many furanoids have been relevant with adverse events, including hepatotoxicity, pulmonary toxicity, and carcinogenesis, possibly in part originating from the *in situ* generation of *cis*-enedial.[31] These reactive species are able to alkylate pivotal cellular proteins and/or DNA. Our previous study showed that the electrophilic reactive metabolites of DBB and EEA could modify lysine and cysteine residue(s) of hepatic proteins to form pyrrole and pyrrolinone derivatives, possibly correlated with the hepatotoxicities of DBB and EEA.[22,23] It has been reported that furan is bioactivated to produce *cis*-2-butene-1,4-dial mediated by cytochrome P450 2E1 This metabolite could react with the exocyclic and endocyclic nitrogens of dCyd, dAdo, and dGuo to produce relatively stable diastereomeric oxadiazabicyclo[3.3.0]octa-imine adducts, thought to be an important mechanism of triggering the toxicities.[18,24] This encouraged us to study the interaction of the *cis*-enedial intermediates derived from DBB and EEA with DNA.

As an initial step, we chemically synthesized the reactive intermediates of DBB and EEA by oxidation of DBB and EEA with DMDO, followed by reaction with dCyd, dGuo, dAdo, or thymine. DBB-derived dCyd, dGuo, and dAdo adducts (A1-A3), EEA-derived dCyd, dGuo, and dAdo adducts (A4-A6) were observed in the corresponding chemical reaction mixtures. However, no such adducts were detected in the reactions of thymine with the reactive metabolites derived from DBB and EEA were observed, presumably due to the lack of exocyclic nitrogen in thymine. Given together, the reactive metabolites of DBB and EEA were able to react with the exocyclic and endocyclic nitrogens of dCyd, dGuo, and dAdo to produce oxadiazabicyclo[3.3.0]octene adducts (**3**, **4**, **5** and **8**, **9**, **10**; Scheme 3 and 4). However, the dAdo and dGuo adducts rapidly rearrange by dehydration to form substituted etheno adducts which contain a reactive aldehydic group (**6**, **7** and **11**, **12**; Scheme 3 and 4). As a consequence, the substituted etheno adducts were found as the primary products of the above reactions. It has been reported that reaction pH is a major factor to determine the rearrangement of the dGuo and dAdo adducts, and they may readily rearrange at pH 7 or 8. Thus, it is most likely that the adducts of dGuo and dAdo mainly exist in the form of etheno adducts under physiological conditions.[19] Interestingly, for the dCyd adducts, this aldehydic form of the adduct preferentially to produce the corresponding cyclic hemiacetal by ring closure (**5** and **10**; Scheme 3 and 4). These observations were consistent with the interactions of the reactive metabolite of furan with dCyd, dGuo, and dAdo.[31]

On the basis of these structures, a general reaction mechanism may be proposed

as follows. Initially, the *cis*-enedial intermediates derived from DBB and EEA reacts with the exocyclic nitrogen atom of the nucleosides (N^4 of dCyd, N^2ofdGuo, and N^6 of dAdo; Scheme 5) to form α, β-unsaturated aldehyde. The double bond derived from the resulting α, β-unsaturated aldehyde reacts with the adjacent endocyclic nitrogen atom (N^3 of dCyd, and N^1 of dGuo, and dAdo; Scheme 5) by 1,4-addition. The final product may be generated from the subsequent attack of the aliphatic hydroxyl group on the second aldehyde group. Alternatively, the reaction mechanism cannot be ruled out, which involves the reaction of the endocyclic nitrogen with reactive intermediates of DBB and EEA, followed by reaction of the exocyclic nitrogen with the terminal aldehyde.

To further characterize the interaction of the *cis*-enedial reactive intermediates derived from DBB and EEA with DNA, we employed calf thymus DNA as a model DNA. Synthetic reactive intermediates derived from DBB and EEA were incubated with calf thymus DNA, followed by treatment with hydrolytic enzymes. Three DBB-derived adducts and three EEA-derived adducts were produced after enzymatic hydrolysis of the resulting DNA adducts. The observed adducts shared the same chromatographic properties as those of A1-A3 and A4-A6, respectively (Figure1C-3C and Figure 4C-6C), suggesting the reactive metabolites of DBB and EEA could covalently bind to calf thymus DNA.

The etheno-dGuo and etheno-dAdo adducts (**6**, **7** and **11**, **12**) with the aldehyde group may be reactive to DNA, which possibly has important implications for the toxicities induced by DBB and EEA. As a result of reactions at the exposed

aldehyde functionalities, these adducts possibly result in the formation of additional products. It has been reported that etheno-dGuo and etheno-dAdo adducts may induce point mutations. It was proposed that these adducts might also further react with nucleophiles of protein and/or DNA, due to the reactive aldehyde functionality, to form the corresponding cross-links. A number of α, β-unsaturated aldehydes and dialdehydes can reportedly cause DNA damage by cross-linkage.[32-36] In addition to cytotoxicity, the cross-link formation may induce large scale deletions or chromosomal rearrangements, which possibly initiates tumors.[38,39] As a consequence, the generation of etheno-dAdo and etheno-dGuo adducts is likely to contribute to the toxicities of DBB and EEA. Future studies will evaluate the toxicological importance of these adducts in animals administered DBB/EEA and the biological activity of these adducts in mutagenesis assays.

In conclusion, the reactive metabolites of DBB and EEA covalently bind to the exocyclic and endocyclic nitrogens of dCyd, dGuo, and dAdo. The reactive metabolites of DBB and EEA also modified dGuo, dAdo, and dCyd of calf thymus DNA. Characterizing the potential DNA modifications by DBB and EEA may be an important step in understanding DBB and EEA-induced hepatotoxicities.

Footnotes. This work was supported in part by the National Natural Science Foundation of China [Grant 81373471, 81430086, 81773813] and University Student Innovation Project [2018116].

Supporting Information Available

Description of mass spectrometric profiling data of dCyd, dGuo, and dAdo adducts derived from DBB/EEA. Description of ^{1}H NMR and ^{13}C NMR Data of DBB-derived dGuo and DBB-derived dAdo adducts in DMSO-d*6*. This material is available free of charge via the Internet at http://pubs.acs.org.

Conflict of interest. The authors declare that there are no conflicts of interest.

Abbreviations

ALT,alanine transaminase; AST, aspartate transaminase; BDA, *cis*-2-butene-1,4-dial; CE, collision energy; CXP, collision cell exit potential; dAdo, 2'-deoxyadenosine; DB, *Dioscoreabulbifera* L.; dCyd, 2'-deoxycytidine; dGuo, 2'-deoxyguanosine; DMDO, Dimethyldioxirane; DBB, Diosbulbin B; DP, declustering potential; EEA, 8-epidiosbulbin E acetate; NMR, nuclear magnetic resonance.

References

[1] Li. S., Iliya. I. A., Deng. J., Zhao. S. (2000) Flavonoids and anthraquinone from *Dioscorea bulbifera* L. *Chin. J. Chin. Mater. Med. 25,* 159-160.

[2] Gao. H.Y., Shui. A. L., Chen. Y. H., Zhang. X. Y., Wu. L. J. (2003) The chemical compositions of *Dioscorea bulbifera* L.J. Shenyang Pharm. Univ. *20,* 178-180.

[3] Grynberg. N. F., Echevarria. A., Lima. J. E., Pamplona. S. S., Pinto. A. C., Maciel, M. A. (1999) Anti-tumour activity of two 19-nor-clerodane diterpenes, trans-dehydrocrotonin and trans-crotonin, from Croton cajucara. *Planta. Med. 65,* 687-689.

[4] Cifuente, D. A., Borkowski, E. J., Sosa, M. E., Gianello, J. C., Giordano, O. S., Tonn, C. E. (2002) Clerodane diterpenes from Baccharis sagittalis: insect antifeedant activity. *Phytochemistry 61*, 899-905.

[5] Demetzos. C., Dimasm. K., Hatziantoniou. S., Anastasaki. T., Angelopoulou D. (2001) Cytotoxic and anti-inflammatory activity of labdane and *cis*-clerodane type diterpenes. *Planta. Med. 67,* 614-618.

[6] Teponno, R. B., Tapondjou, A. L., Gatsing, D., Djoukeng, J. D., Abou-Mansour, E., Tabacchi, R., Tane, P., Stoekli-Evans. H, Lontsi, D. (2006) Bafoudiosbulbins A, and B, two anti-salmonellal clerodane diterpenoids from *Dioscorea bulbifera* L. var. sativa. *Phytochemistry 67,* 1957-1963.

[7] Tang, Y. X. (1995) The research of *Dioscoreae bulbifera* L. in clinical application. *Chin. J. Chin. Mater. Med. 20,* 435-438.

[8] Rasikari, H. L., Leach, D. N., Waterman, P. G., Spooner-Hart, R. N., Basta, A. H., Banbury, L. K., Winter, K. M., Forster, P. I. (2005) Cytotoxic clerodane diterpenes from Glossocarya calcicola. *Phytochemistry 66,* 2844-2850.

[9] Niu, Z. M. and Chen, A. Y. (1994) 16 cases report of toxic hepatitis caused by *Dioscoreabulbifera*. *Chin. J. Integr. Tradit. Western Liver Dis. 4,* 55-56.

[10] Yang, H., Li, J., Cui, X., Yang, C., Li, L., Liu-Clin, J., Misther, M. (2006) Clinical use and adverse drug reaction of compound prescription of *Dioscorea bulbifera* L. in clinical trial. *Clin. Misdiagn Misther 19,* 85-87.

[11] Liu, J. R. (2002) Two cases of toxic hepatitis caused by *Dioscorea Bulbifera* L. *Adverse Drug React. 2,* 129-130.

[12] Wang, J., Ji, L., Liu, H., Wang, Z. (2010) Study of the hepatotoxicity induced by *Dioscorea bulbifera* L. rhizome in mice. *BioSci. Trends 4,* 79-85.

[13] Zhang, H. M. and Yuan, J. Y. (2009) The progress of diosbulbin B research on pharmacology and toxicology. *Chin. Med. Her. 28,* 490-492.

[14] Gao, H., Kuroyanaqi, M., Wu, L., Kawahara, N., Yasuno, T., Nakamura, Y. (2002) Antitumor-promoting constituents from *Dioscorea bulbifera* L. in JB6 mouse epidermal cells. *Biol. Pharm. Bull 25,* 1241-1243.

[15] Lin. D. J., Guo, X. C., Gao, H. Y., Cheng, L., Cheng, M. S., Song, S. J., Peng, Y. and Zheng, J. (2015) *In vitro* and *in vivo* studies of the metabolic activation of 8-epidiosbulbin E acetate. *Chem. Res. Toxicol. 28,* 1737-1746.

[16] Lin, D. J., ,W. W., Peng, Y., Jiang, C. F., Xu, Y. J., Gao, H. Y. and Zheng, J. (2016) Role of metabolic activation in 8-epidiosbulbin E acetate-induced liver

injury: mechanism of action of the hepatotoxic furanoid. *Chem. Res. Toxicol. 29,* 359-366.

[17] Lin. D. J., Li, C. Y., Peng, Y., Gao, H. Y., Zheng, J. (2014) Cytochrome P450-mediated metabolic activation of diosbulbin B. *Drug Metab. Dispos. 42,* 1727-1736.

[18] Byrns, M. C., Predecki, D. P., and Peterson, L. A. (2002) Characterization of nucleoside adducts of *cis*-2-butene-1,4-dial, a reactive metabolite of furan. *Chem. Res. Toxicol. 15,* 373-379.

[19] Byrns, M. C., Vu, C. C., and Peterson, L. A. (2004) The formation of substituted 1, N_6-etheno-2′-deoxyadenosine and 1, N_2-etheno-2′-deoxyguanosine adducts by *cis*-2-butene-1,4-dial, a reactive metabolite of furan. *Chem. Res. Toxicol. 17,* 1607-1613.

[20] Byrns. M. C., Vu, C. C., Neidigh, J. W., Abad, J. L., Jones, R. A., and Peterson, L. A. (2006) Detection of DNA adducts derived from the reactive metabolite of furan *cis*-2-butene-1,4-dial. *Chem. Res. Toxicol. 19,* 414-420.

[21] Chen, L. J., Hecht, S. S., and Peterson, L. A. (1997) Characterization of amino acid and glutathione adducts of *cis*-2-butene-1,4-dial, a reactive metabolite of furan. *Chem. Res. Toxicol. 10,* 866-874.

[22] Lin, D. J., Wang, K., Guo, X. C., Gao, H. Y., Peng, Y., Zheng, J. (2016) Lysine- and cysteine-based protein adductions derived from toxic metabolites of 8-epidiosbulbin E acetate. *Toxicol. Lett. 264,* 20-28.

[23] Wang, K., Lin, D. J., Guo, X. C., Huang, W. L., Peng, Y. and Zheng, J. (2017) Chemical identity of interaction of protein with reactive metabolite of diosbulbin B *in vitro* and *in vivo*. *Toxins* 9, 249

[24] Gingipalli, L., and Dedon, P. C. (2001) Reaction of *cis*- and trans-2-butene-1,4-dial with 2′-deoxycytidine to form stable oxadiazabicyclooctaimine adducts. *J. Am. Chem. Soc. 123,* 2664-2665.

[25] Neuwirth, C., Mosesso, P., Pepe, G., Fiore, M., Malfatti, M., Turteltaub, K., Dekant, W., and Mally, A. (2012) Furan carcinogenicity: DNA binding and genotoxicity of furan in rats *in vivo*. *Mol. Nutr. Food Res. 56,* 1363-1374.

[26] Kawasaki, T., Komori, T., Setoguchi, S. (1968) Furanoid norditerpenes from *Dioscoreacae* plants. I. Diosbulins A, B, and C from *Dioscorea bulbifera* L. forma spontanea Makino et Nemoto. *Chem. Pharm. Bull 16,* 2430-2435.

[27] Shrirama, V., Jahagirdarb, S., Lathac, C., Kumara, V., Puranikd, V., Rojatkard, S., Dhakephalkar, P. K., and Shitole, M. G. (2008) A potential plasmid-curing agent, 8-epidiosbulbin E acetate, from *Dioscorea bulbifera* L. against multidrug-resistant bacteria. *Int. J. Antimicrob Ag. 32,* 405-410.

[28] Taber, D. F., DeMatteo, P. W., and Hassan, R. A. (2013) Simplified preparation of dimethyldioxirane (DMDO). *Org. Synth. 90,* 350-357.

[29] Adam, W., Chan, Y. Y., Cremer, D., Gauss, J., Scheutzow, D., Scheutzow, D., Schindler, M. J. (1987) Spectral and chemical properties of dimethyldioxirane as determined by experiment and ab initio calculations. *Org. Chem. 52,* 2800-2803.

[30] Li, W. W., Lin, D. J., Gao, H. Y., Xu, Y. J., Smith, C. V., Peng, Y., and Zheng J. (2016) Metabolic activation of the furan moiety makes diosbulbin B hepatotoxic. *Arch. Toxicol. 90,* 863-872.

[31] Peterson, L. A. (2013) Reactive metabolites in the biotransformation of molecules containing a furan ring. *Chem. Res. Toxicol. 26,* 6-25.

[32] Kozekov, I. D., Nechev, L. V., Sanchez, A., Harris, C. M., Lloyd, R. S., and Harris, T. M. (2001) Interchain cross-linking of DNA mediated by the principal adduct of acrolein. *Chem. Res. Toxicol. 14,*1482-1485.

[33] Kozekov, I. D., Nechev, L. V., Moseley, M. S., Harris, C. M., Rizzo, C. J., Stone, M. P., and Harris, T. M. (2003) DNA interchain crosslinks formed by acrolein and crotonaldehyde. *J. Am. Chem. Soc. 125,*50-61.

[34] Kurtz, A. J., and Lloyd, R. S. (2003) 1,N_2-deoxyguanosine adducts of acrolein, croton aldehyde, and trans-4-hydroxynonenal crosslink to peptides via Schiff base linkage. *J. Biol. Chem. 278,* 5970-5976.

[35] Kuykendall, J. R., and Bogdanffy, M. S. (1992) Efficiency of DNA histone cross-linking induced by saturated and unsaturated aldehydes *in vitro*. *Mutat. Res. 283,*131-136.

[36] Niedernhofer, L. J., Riley, M., Schnetz-Boutaud, N., Sanduwaran, G., Chaudhary, A. K., Reddy, G. R., and Marnett, L. J. (1997) Temperature-dependent formation of a conjugate between tris-(hydroxymethyl) amino methane buffer and the malondialdehyde-DNA adduct pyrimido purinone. *Chem. Res. Toxicol. 10,*556-561.

[38] Greenberg, R. B., Alberti, M., Hearst, J. E., Chua, M.A., and Saffran, W. A. (2001) Recombinational and mutagenic repair of psoralen interstrand cross-links in Saccharomyces cerevisiae. *J. Biol. Chem. 276,* 31551-31560.

[39] Speit, G. and Merk, O. (2002) Evaluation of mutagenic effects of form aldehyde in vitro: Detection of cross-links and mutations in mouse lymphoma cells. *Mutagenesis 17,* 183-187.

Figure Legends

Figure 1. LC-MS MRM analysis of A1 (*m*/*z* 588–472) in (A) DBB was oxidized by DMDO, followed by the reaction with dCydand(B) DBB was oxidized by DMDO, followed by the reaction withcalf thymus DNAand then DNA digestion. (C) The MS/MS spectrum of DBB-derived dCyd adduct (A1).

Figure 2. LC-MS MRM analysis of A2 (*m*/*z* 610–494) in (A) DBB was oxidized by DMDO, followed by the reaction with dGuoand(B) DBB was oxidized by DMDO, followed by the reaction withcalf thymus DNAand then DNA digestion. (C) The MS/MS spectrum of DBB-derived dGuo adduct (A2).

Figure 3. LC-MS MRM analysis of A3 (*m*/*z* 594–478) in (A) DBB was oxidized by DMDO, followed by the reaction with dAdoand(B) DBB was oxidized by DMDO, followed by the reaction withcalf thymus DNA, and then DNA digestion. (C) The MS/MS spectrum of DBB-derived dAdo adduct (A3).

Figure 4. LC-MS MRM analysis of A4 (*m*/*z* 632–456) in (A) EEA was oxidized by DMDO, followed by the reaction with dCydand(B) EEA was oxidized by DMDO, followed by the reaction withcalf thymus DNAand then DNA digestion. (C) The MS/MS spectrum of EEA-derived dCyd adducts (A4).

Figure 5. LC-MS MRM analysis of A5 (*m*/*z* 654–478) in (A) EEA was oxidized by DMDO, followed by the reaction with dGuoand(B) EEA was oxidized by DMDO, followed by the reaction with calf thymus DNAand then DNA digestion. (C) The MS/MS spectrum of EEA-derived dGuo adduct (A5).

Figure 6. LC-MS MRM analysis of A6 (*m*/*z* 638→462) in (A) EEA was oxidized

by DMDO, followed by the reaction withdAdoand(B) EEA was oxidized by DMDO, followed by the reaction withcalf thymus DNAand then DNA digestion. (C) The MS/MS spectrum of EEA-derived dAdo adduct (A6).

Scheme 1. Structures of DBB, EEA, DBB-*cis*-enedial, and DBB-*cis*-enedial.

Scheme 2. Structures of DBB-derived dCyd, dGuo, and dAdo adducts.

Scheme 3. Proposed reaction mechanism of DBB-derived *cis*-enedial with DNA bases.

Scheme 4. Proposed reaction mechanism of EEA-derived *cis*-enedial with DNA bases.

Scheme 5. Proposed mechanisms for the formation of DBB/EEA-*cis*-enedial-DNA adducts

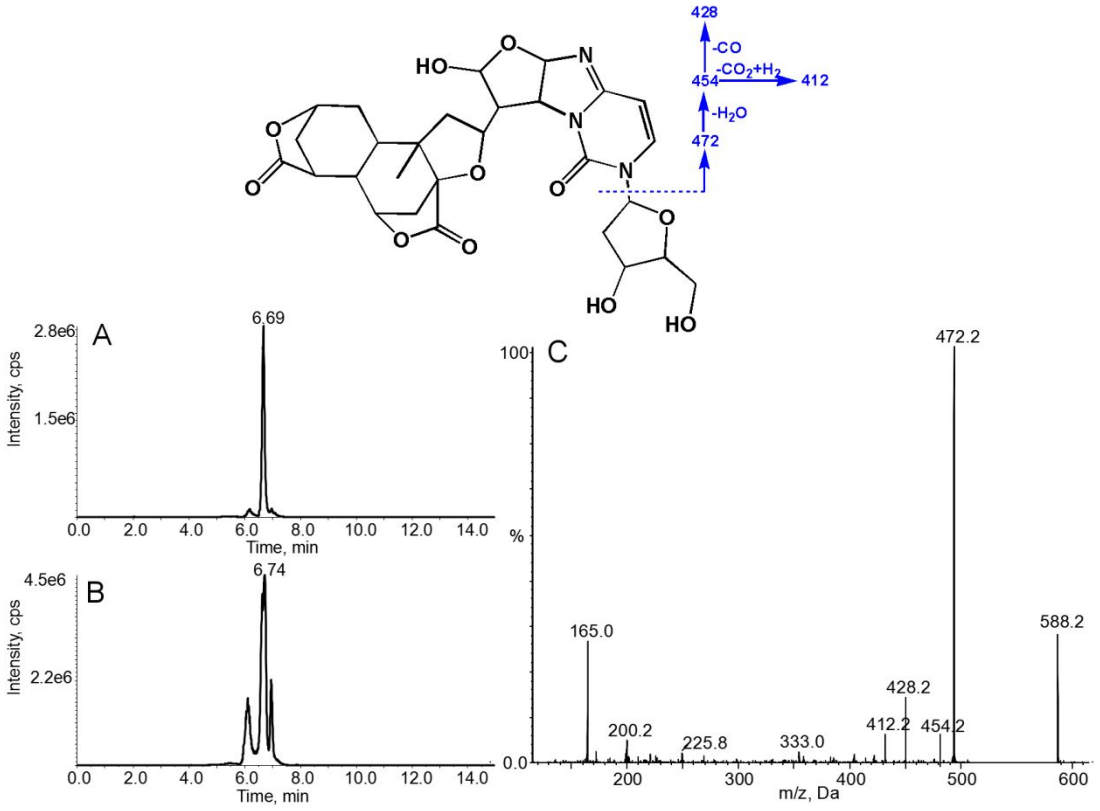

Figure 1. LC-MS MRM analysis of A1 (*m*/*z* 588–472) in (A) DBB was oxidized by DMDO, followed by the reaction with dCyd and(B) DBB was oxidized by DMDO, followed by the reaction with calf thymus DNA and then DNA digestion. (C) TheMS/MS spectrum of DBB-derived dCyd adduct (A1).

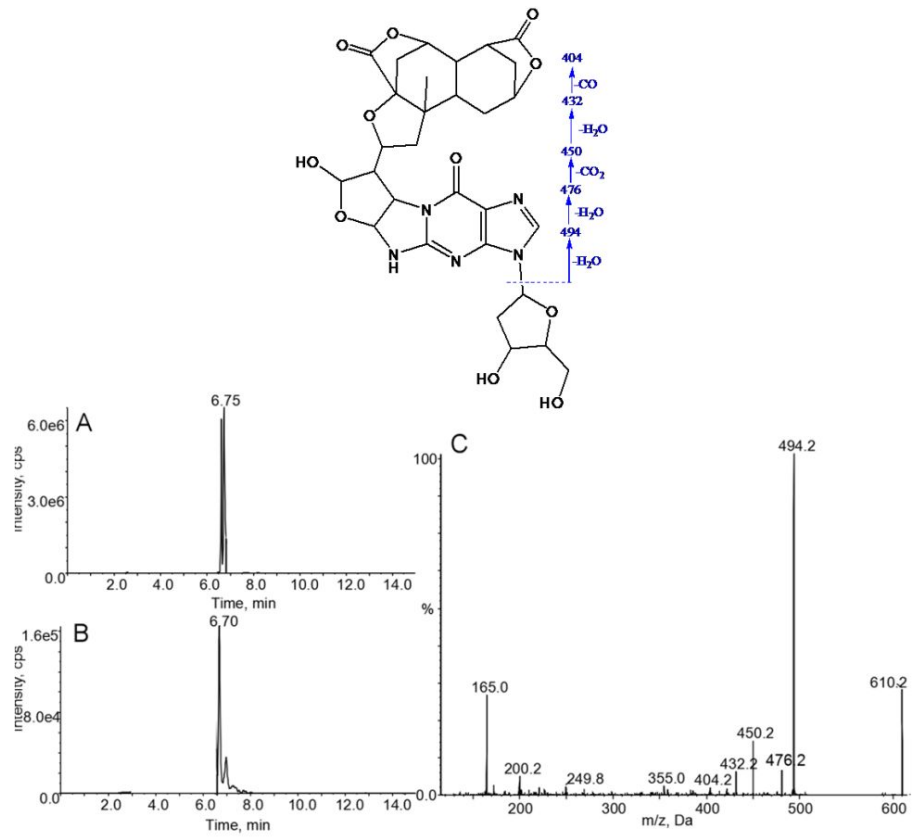

Figure 2. LC-MS MRM analysis of A2 (*m*/*z* 610–494) in (A) DBB was oxidized by DMDO, followed by the reaction with dGuo and(B) DBB was oxidized by DMDO, followed by the reaction with calf thymus DNA and then DNA digestion. (C) The MS/MS spectrum of DBB-derived dGuo adduct (A2).

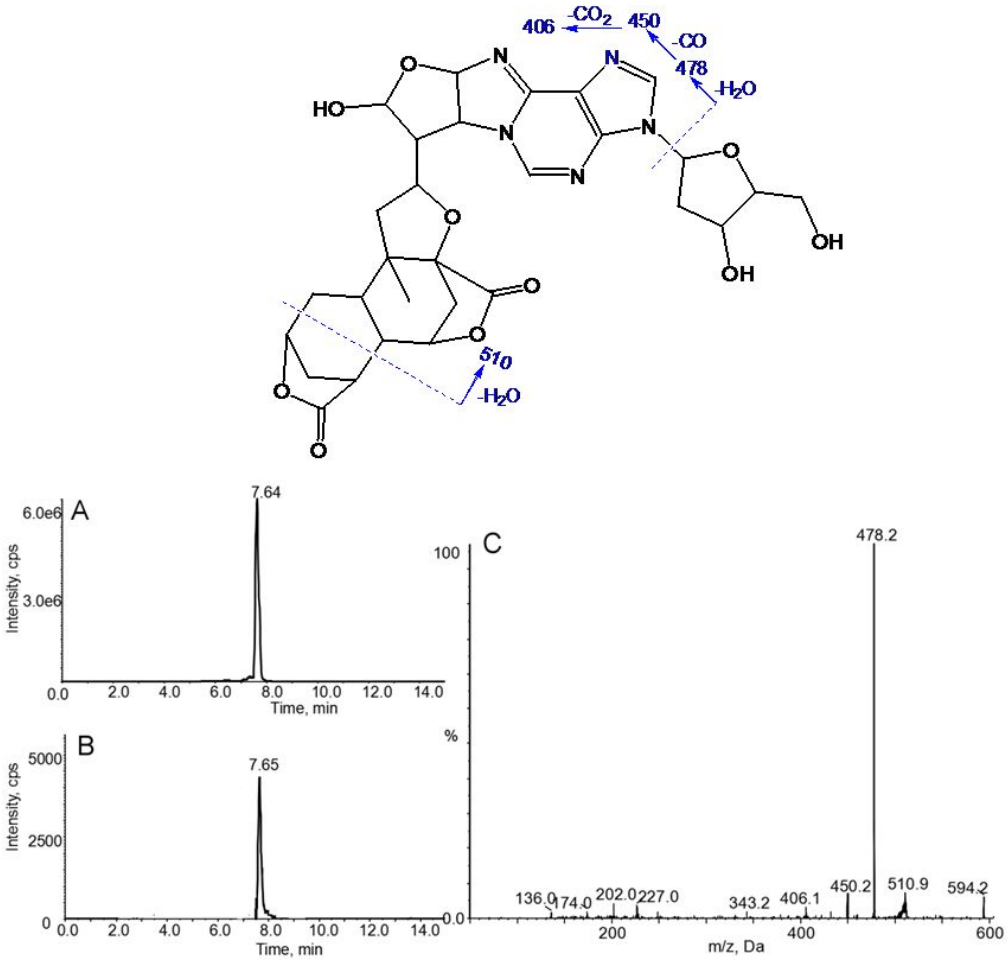

Figure 3. LC-MS MRM analysis of A3 (*m*/*z* 594–478) in (A) DBB was oxidized by DMDO, followed by the reaction with dAdo and (B) DBB was oxidized by DMDO, followed by the reaction with calf thymus DNA, and then DNA digestion. (C) The MS/MS spectrum of DBB-derived dAdo adduct (A3).

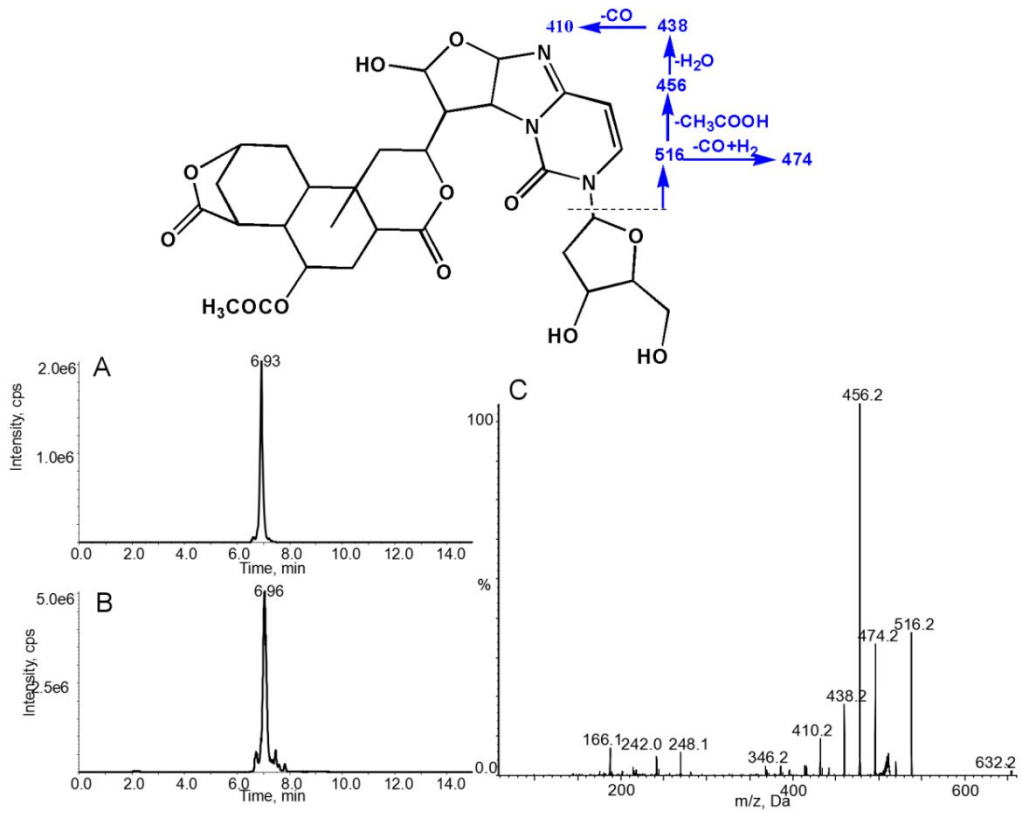

Figure 4. LC-MS MRM analysis of A4 (*m*/*z* 632–456) in (A) EEA was oxidized by DMDO, followed by the reaction with dCyd and (B) EEA was oxidized by DMDO, followed by the reaction with calf thymus DNA and then DNA digestion. (C) The MS/MS spectrum of EEA-derived dCyd adducts (A4).

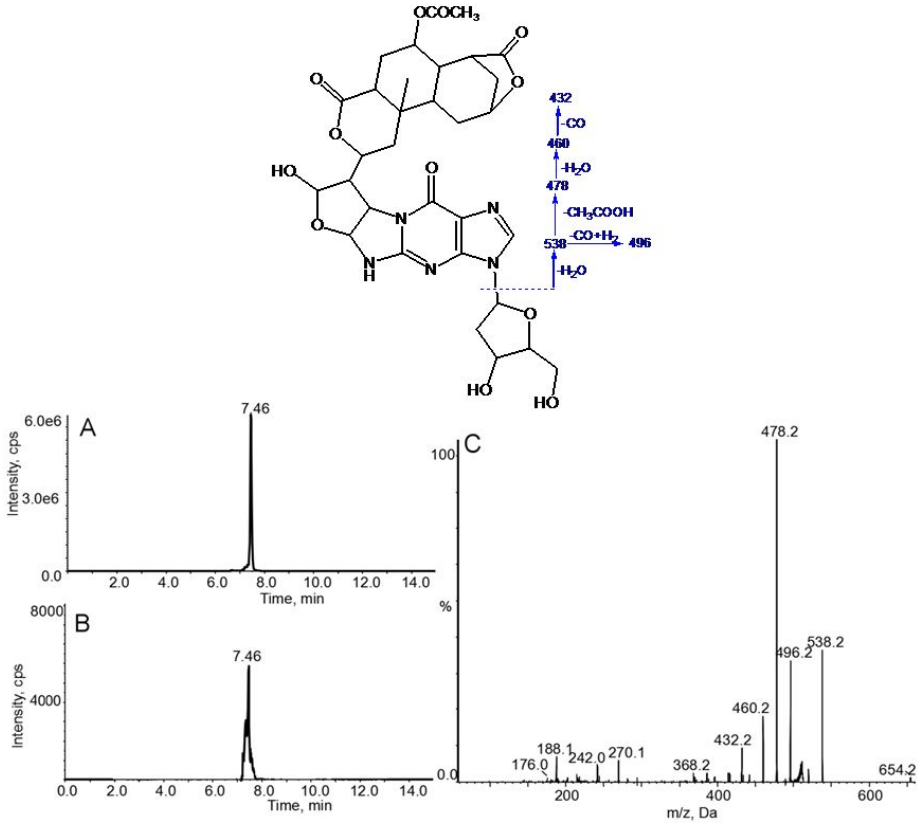

Figure 5. LC-MS MRM analysis of A5 (*m*/*z* 654–478) in (A) EEA was oxidized by DMDO, followed by the reaction with dGuo and (B) EEA was oxidized by DMDO, followed by the reaction with calf thymus DNA and then DNA digestion. (C) The MS/MS spectrum of EEA-derived dGuo adduct (A5).

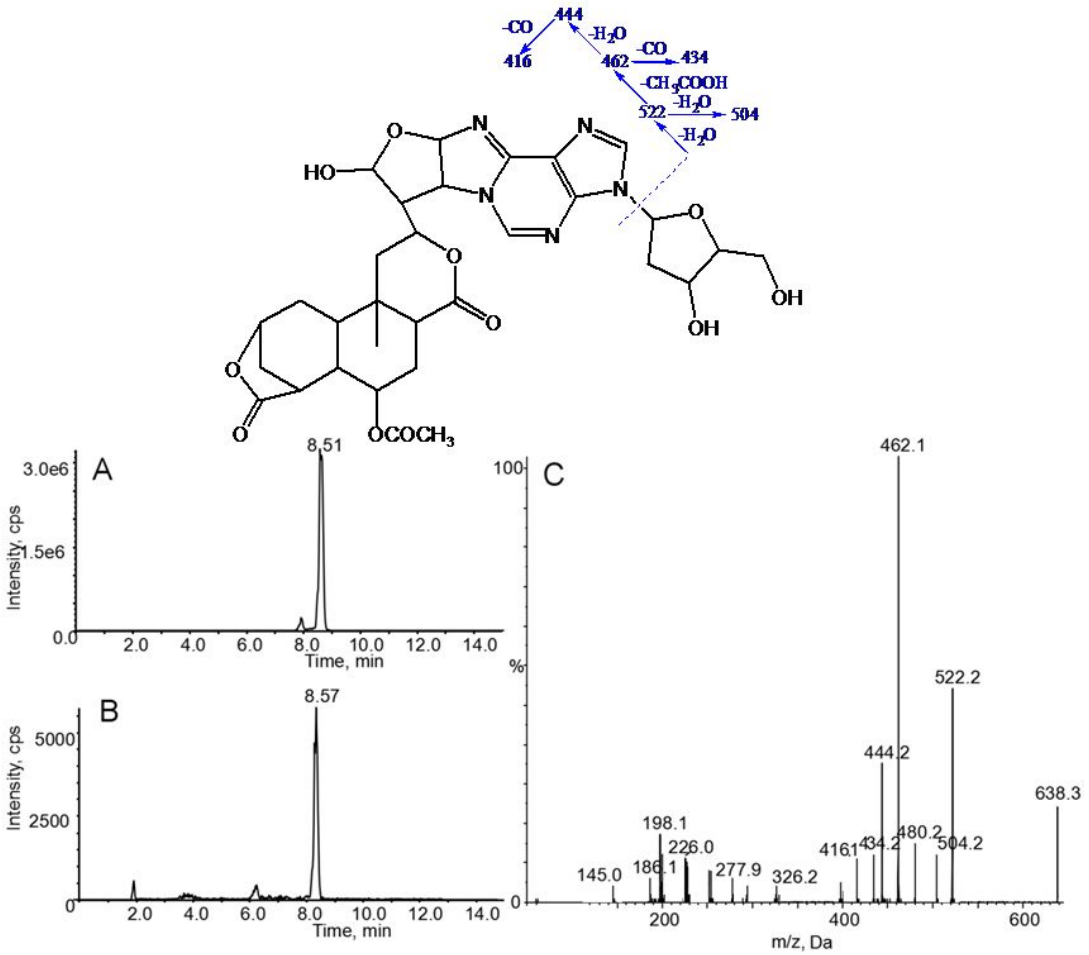

Figure 6. LC-MS MRM analysis of A6 (*m*/*z* 638→462) in (A) EEA was oxidized by DMDO, followed by the reaction with dAdo and (B) EEA was oxidized by DMDO, followed by the reaction with calf thymus DNA and then DNA digestion. (C) The MS/MS spectrum of EEA-derived dAdo adduct (A6).

Scheme 1. Structures of DBB, EEA, DBB-*cis*-enedial, and DBB-*cis*-enedial.

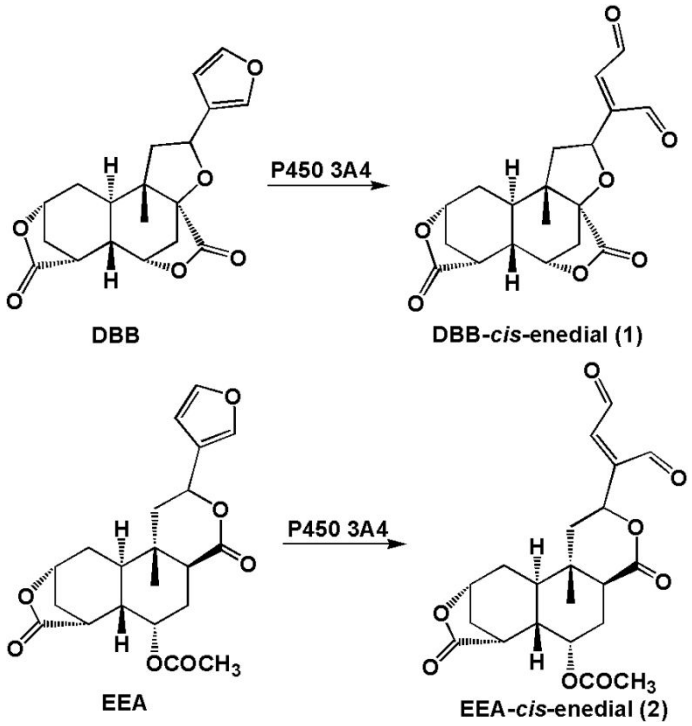

Scheme 2. Structures of DBB-derived dCyd, dGuo, and dAdo adducts.

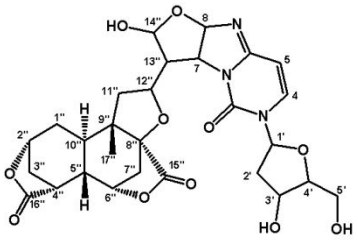

DBB-derived dCyd adduct

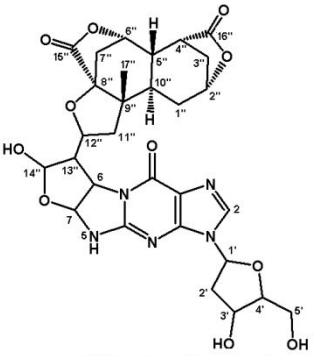

DBB-derived dGuo adduct

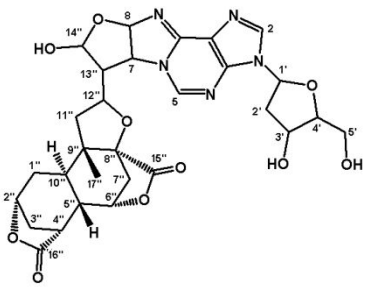

DBB-derived dAdo adduct

Scheme 3. Proposed reaction mechanism of DBB-derived *cis*-enedial with DNA bases.

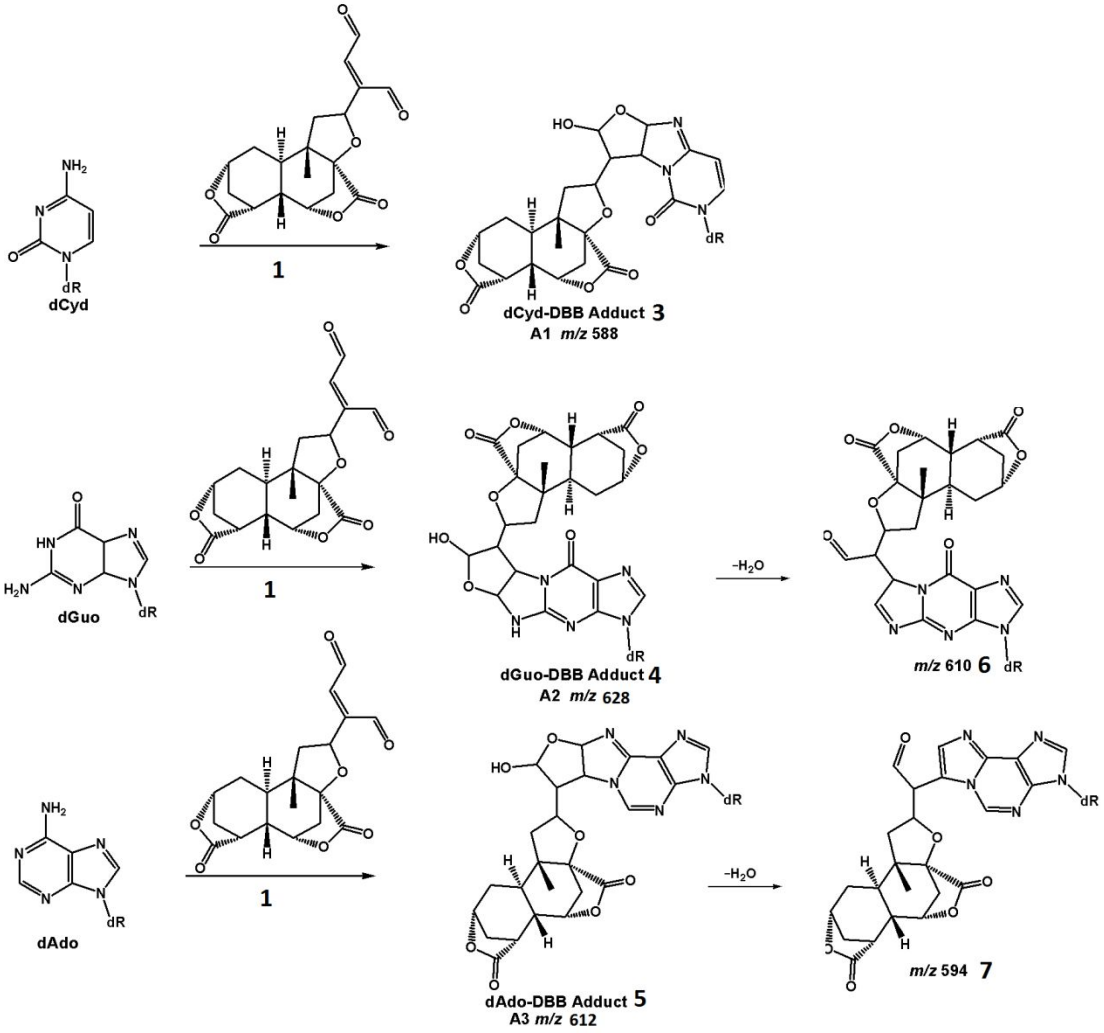

dR = 2'-deoxyribose

Scheme 4. Proposed reaction mechanism of EEA-derived *cis*-enedial with DNA bases.

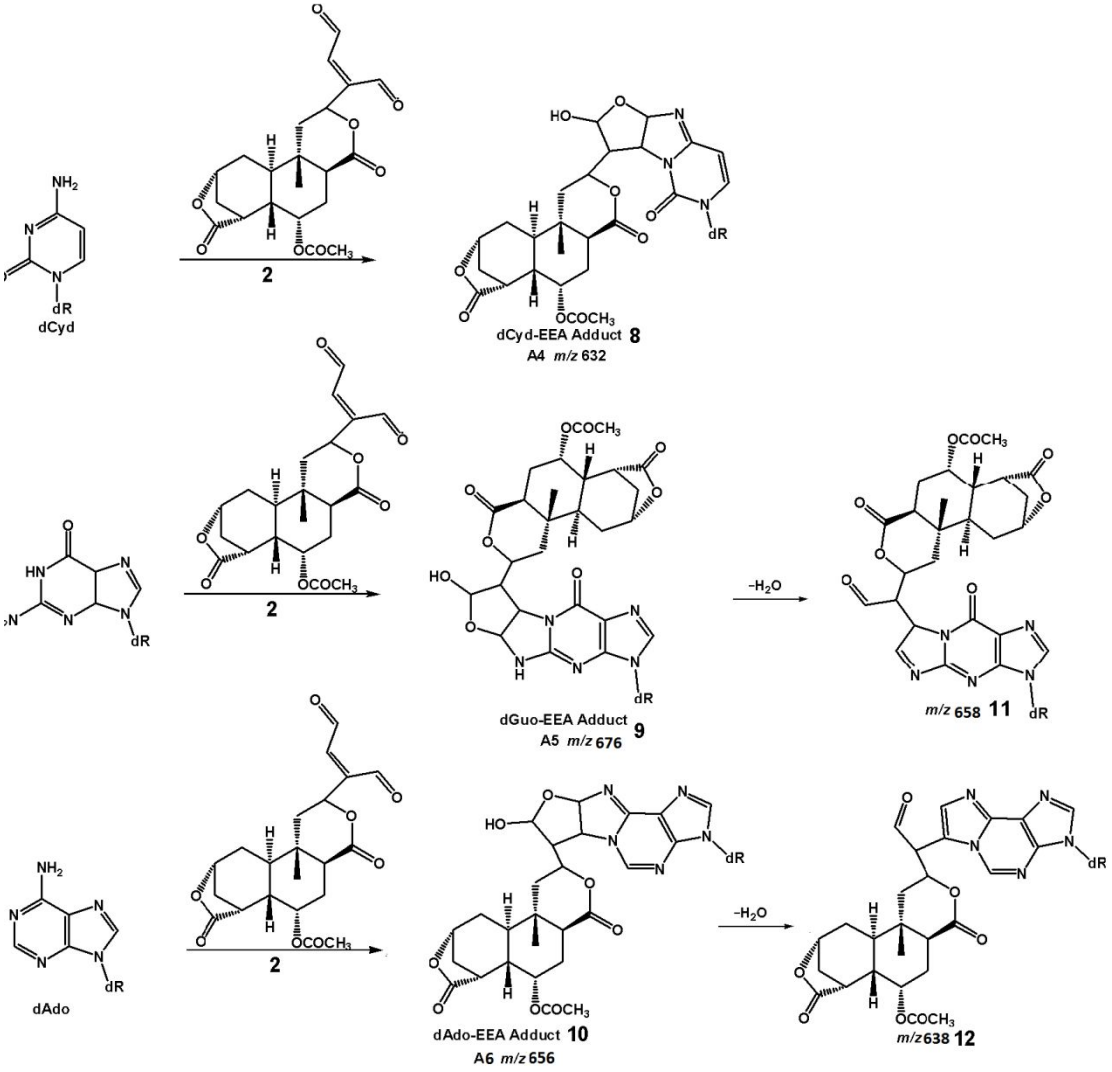

dR = 2'-deoxyribose

Scheme 5. Proposed mechanisms for the formation of DBB/EEA-*cis*-enedial-DNA adducts.

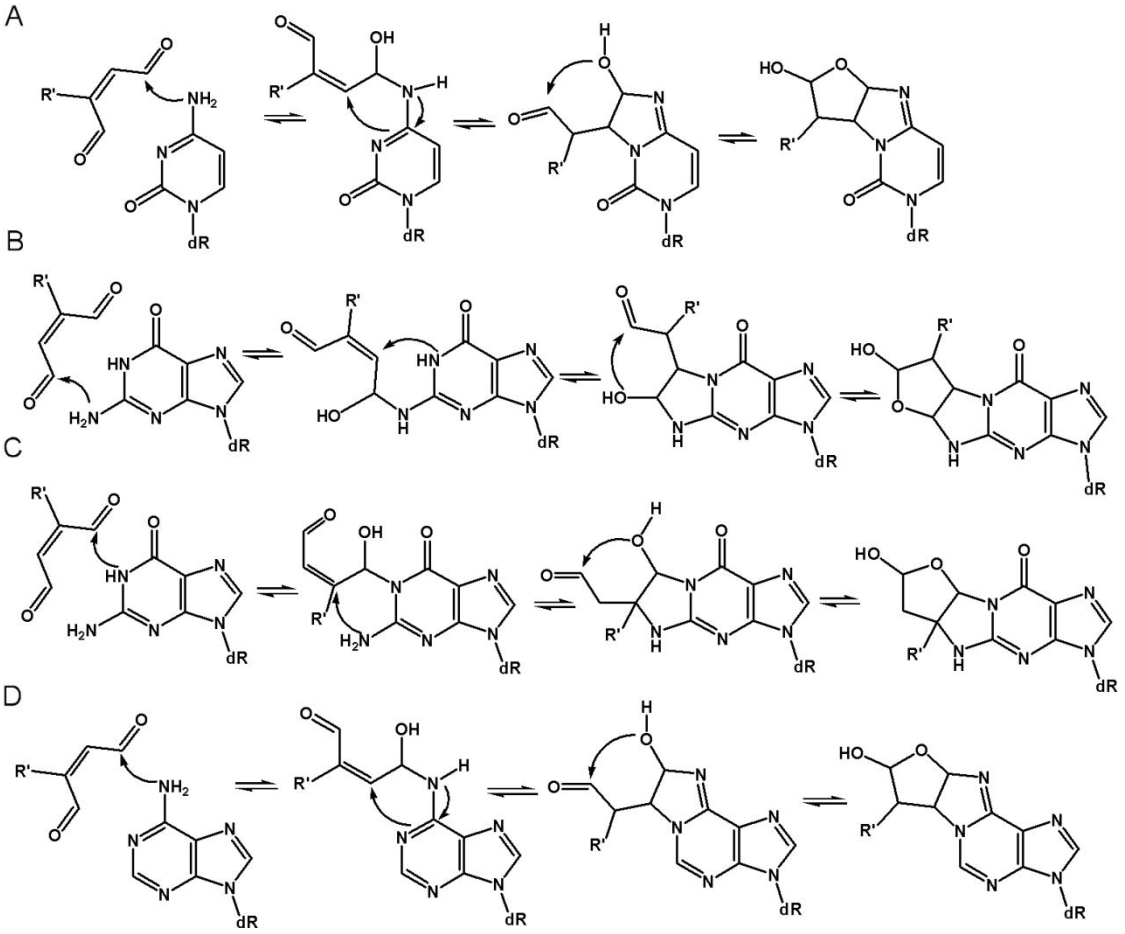

(A)dCyd; (B) dGuo; (C) dAdo; dR = 2'-deoxyribose; R'= 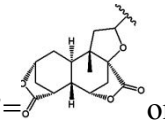 or